Candidate New Rotavirus Species in Sheltered Dogs, Hungary

Eszter Mihalov-Kovács, Ákos Gellért, Szilvia Marton, Szilvia L. Farkas, Enikő Fehér, Miklós Oldal, Ferenc Jakab, Vito Martella, Krisztián Bányai

We identified unusual rotavirus strains in fecal specimens from sheltered dogs in Hungary by viral metagenomics. The novel rotavirus species displayed limited genome sequence homology to representatives of the 8 rotavirus species, A–H, and qualifies as a candidate new rotavirus species that we tentatively named *Rotavirus I*.

Rotaviruses (family *Reoviridae*, genus *Rotavirus*) are major causes of acute dehydrating gastroenteritis in birds and mammals (*1*). Rotaviruses have an 11-segmented dsRNA genome encoding 6 structural proteins (viral protein [VP] 1–4, VP6, and VP7) and at least 5 functional nonstructural proteins (NSPs; NSP1–NSP5) (online Technical Appendix Table 1, http://wwwnc.cdc.gov/EID/article/21/4/14-1370-Techapp1.pdf). Traditionally, rotaviruses have been classified into (sero)groups on the basis of major antigenic differences that predominantly reside in the VP6 and of the genomic RNA profile obtained by polyacrylamide gel electrophoresis and silver staining (*1*). Recently, a VP6 gene sequence–based classification scheme has been proposed to replace the conventional methods. An empirical 53% aa identity was demonstrated to reliably distinguish strains of various rotavirus groups (*2*). Also, reclassification of the 8 rotavirus groups as distinct species within the *Rotavirus* genus, designated *Rotavirus A–H*, has been proposed.

Rotavirus A has been detected in a wide variety of mammals and birds. In mammals, both endemic and epidemic forms of rotavirus B, C, E, and H infections have been described, whereas rotavirus D, F, and G have been identified only in birds (*1–3*). Genetically diverse rotaviruses have been found in some viral metagenomics studies (*4*,*5*). Using the metagenomic approach and the VP6-based molecular classification scheme, we found evidence for a novel rotavirus species that we tentatively called *Rotavirus I*.

Author affiliations: Hungarian Academy of Sciences–Centre for Agricultural Research, Budapest, Hungary (E. Mihalov-Kovács, S. Marton, S.L. Farkas, E. Fehér, K. Bányai); Hungarian Academy of Sciences–Centre for Agricultural Research, Martonvásár, Hungary (Á. Gellért); University of Pécs, Pécs, Hungary (M. Oldal, F. Jakab); Università Aldo Moro di Bari, Valenzano, Italy (V. Martella)

DOI: http://dx.doi.org/10.3201/eid2104.141370

The Study

During 2012, we collected fecal specimens from sheltered dogs in northern Hungary to detect enteric viruses. Of 63 samples obtained from 50 animals, 37 randomly selected samples (from 33 animals) were subjected to random primed reverse transcription PCR and semiconductor sequencing by using the Ion Torrent PGM platform (New England Biolabs, Ipswich, MA, USA) (online Technical Appendix). Bioinformatics analysis consisted of the mapping of reads >40 bases against ≈1.7 million viral sequences downloaded from GenBank by applying moderately rigorous mapping parameters (length fraction 0.6; similarity fraction 0.8) within the CLC Genomics Workbench (http://www.clcbio.com/).

One sample (KE135/2012) obtained from a suckling dog in May 2012 was positive for several enteric viruses. When analyzing the initially obtained ≈60.5-K sequence reads, in addition to canine rotavirus A (141 reads), astrovirus (2,399 reads), and parvovirus (3,623 reads), we identified a single 53-nt sequence read that mapped to the VP1 gene of rotavirus B. Another sample, KE528/2012, collected during August 2012 from an adult dog with diarrhea, was positive for coronavirus (30 reads), vesivirus (17 reads), picodicistrovirus (3 reads), and astrovirus (1 read); in addition, 7 and 5 sequence reads, respectively, mapped to the VP1 and VP3 genes of rotavirus H and/or B.

Subsequently, we enriched genomic dsRNA of KE135/2012 by differential LiCl precipitation; however, the enriched dsRNA remained invisible by polyacrylamide gel electrophoresis and silver staining. Because of the apparent low titer of the novel rotavirus, we tried to obtain more sequence data by drastically increasing the output in parallel sequencing runs. De novo assembly of the resulting ≈1.59 million sequence reads readily identified homologs of the structural and some nonstructural genes, which were divergent from rotavirus A–H reference sequences (Table; online Technical Appendix Table 1). Determination of the coding regions in most cases was successful by extension of the termini of consensus sequences using the Ion Torrent sequence reads. However, we found no evidence for NSP3 and NSP4 with this approach, probably because of the great sequence divergence of these genes across members of the genus (*6*,*7*). Because the genomic RNA of each rotavirus species is characterized by low GC (guanine:cytosine) content (29%–40%), we expected that contigs with low GC content and with no GenBank homologs might be good candidates for detecting the missing genes. Indeed, further assembly and subsequent analysis

Table. Sequencing depth for the putative rotavirus I strains obtained by massively parallel sequencing*

	KE135/2012		KE528/2012	
Gene	Mapped read count	Average coverage (X)	Mapped read count	Average coverage (X)
VP1	9632	478	1286	59
VP2	7762	455	860	46
VP3	6361	510	657	49
VP4	5887	436	716	47
VP6	4762	700	582	72
VP7	2841	594	258	45
NSP1	3677	450	561	62
NSP2	2980	529	401	64
NSP3	2528	523	176	32
NSP4	2272	586	229	51
NSP5	1098	387	249	72

*Total sequence reads to obtain genomic RNA sequence for KE135/2012 and KE 528/2012 were 1,591,803, and 144,747, respectively. The minimum overlap with the consensus sequences (i.e., the de novo assembled rotavirus I–specific consensus sequences) was 20 nt, the minimum identity was 80%. To improve the mapping results, the following gap penalties were applied for the dataset: mismatch cost = 2, insertion cost = 3, deletion cost = 3. After visual inspection of the sequence alignments and remapping onto the obtained gene sequence, a single consensus sequence was finalized for each genome segment.

of selected sequence stretches helped to identify the NSP3 by similarity search through the blastx engine (http://blast.ncbi.nlm.nih.gov/Blast.cgi) after an 800-bp long fragment was obtained, and analysis of the structural features of the deduced protein sequence supported detection of the putative NSP4. The obtained consensus sequence was used as reference to map other viral metagenomics data generated from the sheltered dog population; however, except for the aforementioned sample, KE528/2012, we found no additional specimens by this method to contain homologous viruses. The 2 related unusual rotaviruses, KE135/2012 and KE528/2012, had conserved genome segment termini (5′ end, GGC/TA; 3′ end, AACCC) and shared high sequence identities in most genes (e.g., VP2: 88% nt, 95% aa; NSP4: 99% nt, 99% aa) and very low sequence similarity in the VP7 gene (53% nt, 38% aa) (GenBank accession nos. KM369887–KM369908; online Technical Appendix).

The deduced VP6 amino acid sequences served as the basis to classify these 2 unusual rotavirus strains (*2*). The greatest amino acid sequence identity of the VP6 proteins was found when compared to the novel rotavirus H strains (≤46%); lower sequence similarities were found in comparison to randomly selected representatives of other rotvirus species (e.g., rotavirus G and B, ≤37%; rotavirus A, C, D, and F, ≤18%).

To extend the analysis and assess whether the obtained VP6 gene might be functionally integral, we conducted molecular modeling of the amino acid sequence. In brief, amino acid sequence similarity values created a reliable protein model (*8*,*9*) showing similar protein folding of the VP6 monomer and comparable electrostatic charge pattern around the 3-fold axis of the VP6 homotrimer to that experimentally determined for rotavirus A (Figure 1). Subsequent phylogenetic analysis of the VP6 protein identified 2 major clades of rotaviruses (*6*). The novel rotavirus strains

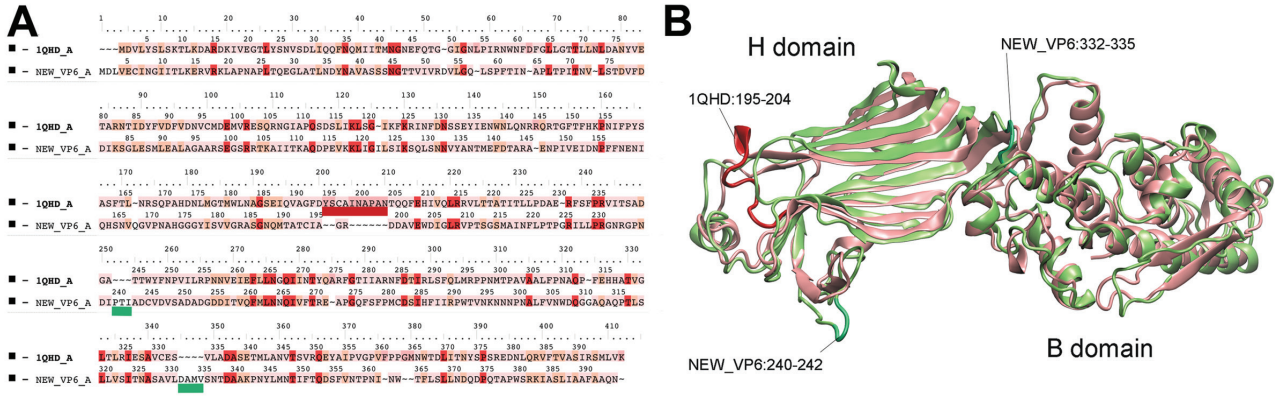

Figure 1. Structure comparison of rotavirus viral protein (VP) 6 proteins. A) Structure-based amino acid sequence alignment of the novel canine rotavirus VP6 protein and the template bovine rotavirus A VP6 protein. The background of the sequence alignments reflects the homology levels of the 2 VP6 sequences. Red, identical amino acid; orange, similar amino acid; pink, different amino acid. The main structural differences are indicated by dark red and menthol green on the sequence alignment and on the superimposed VP6 structures. B) Cartoon presentation of the homologous VP6 proteins: pink, rotavirus A; green, rotavirus I. Further information is available in the online Technical Appendix (http://wwwnc.cdc.gov/EID/article/21/4/14-1370-Techapp1.pdf).

clustered with species H, G, and B within clade 2, whereas clade 1 included representative strains of species A, C, D, and F (Figure 2). This pattern of clustering was also evident when we analyzed the remaining genes. Collectively, sequence and phylogenetic analysis demonstrated moderate genetic relatedness of the unusual canine rotaviruses to representative strains of species A–H, suggesting that they belong to a novel species, tentatively called *Rotavirus I*. The prototype strains were named RVI/Dog-wt/HUN/KE135/2012/G1P1 and RVI/Dog-wt/HUN/KE528/2012/G2P1 according to recent guidelines (*10*) (online Technical Appendix).

Short rotavirus sequences detected recently in the fecal viral flora of cats and California sea lions (*4*,*5*) showed closer relatedness to our strains in the amplified VP6- and VP2-specific stretches, respectively, than to the corresponding genomic regions of reference rotavirus species (VP6, ≈70 aa, 67% vs. <55%; VP2, ≈160 aa, 78%–86% vs. <44%) (online Technical Appendix). These published data (*4*,*5*) together with our results suggest that genetically related non–rotavirus A–H strains occur in various carnivore host species and geographic settings.

Conclusions

We identified 2 representative strains of a novel rotavirus species, *Rotavirus I*. Many questions remain, including those related to the epidemiology, host range, and evolution of this species. One intriguing finding was the distantly related VP7 genes expressed on a fairly conserved genetic backbone. Typically, very low sequence identity values within the VP7 gene (e.g., rotavirus A, as low as 60% nt and 55% aa; rotavirus B, 54% nt, 46% aa; rotavirus H, 63% nt, 56% aa) can be seen when strains from different host species are compared (*11*–*13*). Whether the VP7 gene(s) of rotavirus I strains could have been acquired in the past from another rotavirus species by reassortment remains uncertain, given that reassortment among various rotavirus

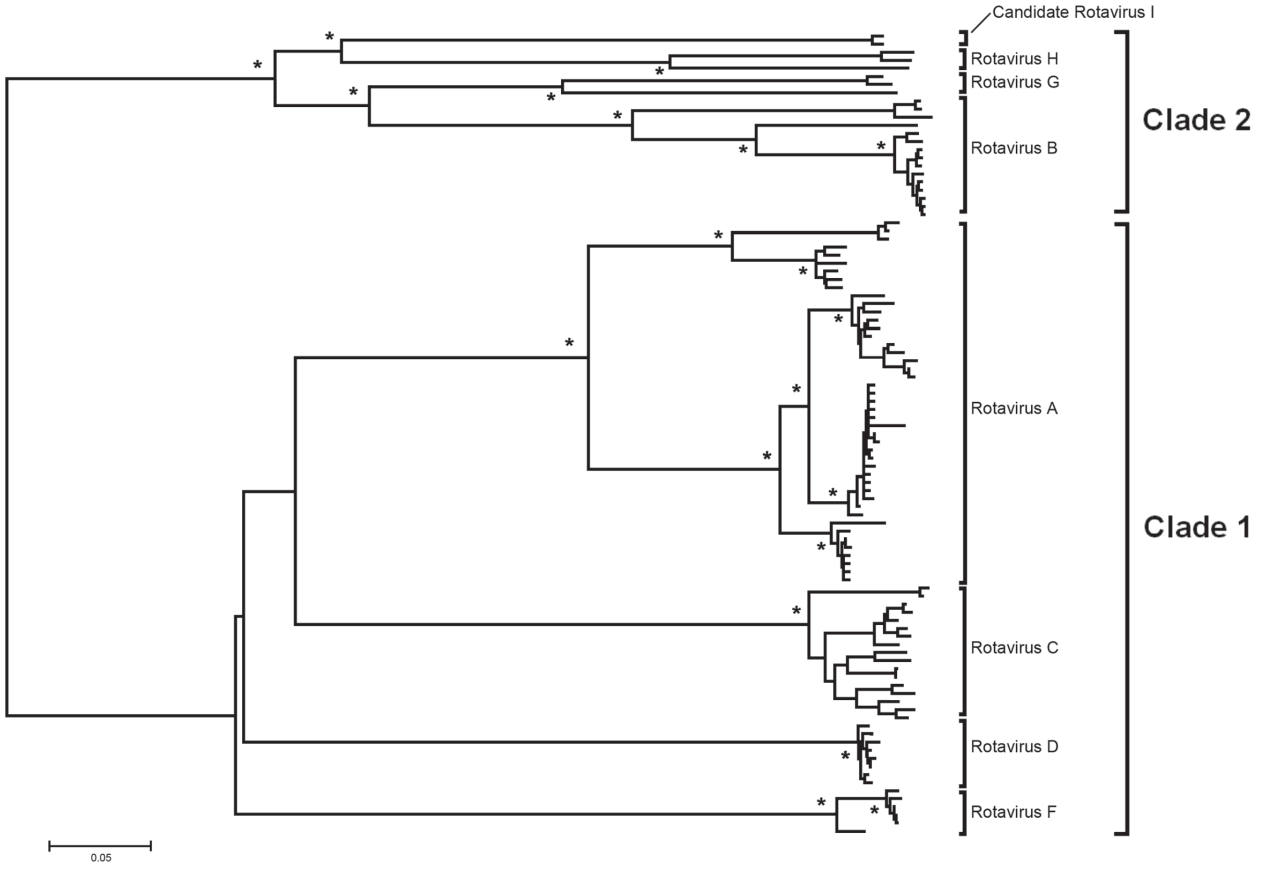

Figure 2. Protein sequence–based phylogenetic tree of the rotavirus viral protein 6 gene obtained by the neighbor-joining algorithm. Asterisks indicate >90% bootstrap values. The 2 canine rotavirus strains from Hungary that belong to the proposed novel *Rotavirus I* cluster with rotavirus H, G, and B within a major clade referred to as clade 2. Rotavirus A, C, D, and F strains belong to clade 1 (*6*). Scale bar indicates nucleotide substitutions per site.

species is thought to occur only rarely (*7*,*14*). Further information is needed to better understand this genetic diversity within rotavirus I.

Financial support was obtained from the Momentum Program (Hungarian Academy of Sciences) and the Hungarian Scientific Research Program (OTKA [Országos Tudományos Kutatási Alapprogramok] 108793; licensing of the Schrödinger Suite software package). Á.G. received a János Bolyai fellowship; F.J. received additional funding from TÁMOP (4.2.4.A/2-11-1-2012-0001).

Dr. Mihalov-Kovács is a PhD student at the Pathogen Discovery Group, Institute for Veterinary Medical Research, Centre for Agricultural Research, Hungarian Academy of Sciences. Her research interests include discovery of novel viruses in domesticated animals.

References

1. Estes MK, Kapikian AZ. Rotaviruses. In: Knipe DM, Howley PM, Griffin DE, Lamb RA, Martin MA, Roizman B, et al., editors. Fields virology. 5th ed. Philadelphia: Lippincott Williams & Wilkins; 2007. p. 1917–74.
2. Matthijnssens J, Otto PH, Ciarlet M, Desselberger U, Van Ranst M, Johne R. VP6-sequence-based cutoff values as a criterion for rotavirus species demarcation. Arch Virol. 2012;157:1177–82. http://dx.doi.org/10.1007/s00705-012-1273-3
3. Marthaler D, Rossow K, Culhane M, Goyal S, Collins J, Matthijnssens J, et al. Widespread rotavirus H in commercially raised pigs, United States. Emerg Infect Dis. 2014;20:1195–8. http://dx.doi.org/10.3201/eid2007.140034
4. Ng TF, Mesquita JR, Nascimento MS, Kondov NO, Wong W, Reuter G, et al. Feline fecal virome reveals novel and prevalent enteric viruses. Vet Microbiol. 2014;171:102–11. http://dx.doi.org/10.1016/j.vetmic.2014.04.005
5. Li L, Shan T, Wang C, Côté C, Kolman J, Onions D, et al. The fecal viral flora of California sea lions. J Virol. 2011;85:9909–17. http://dx.doi.org/10.1128/JVI.05026-11
6. Kindler E, Trojnar E, Heckel G, Otto PH, Johne R. Analysis of rotavirus species diversity and evolution including the newly determined full-length genome sequences of rotavirus F and G. Infect Genet Evol. 2013;14:58–67. http://dx.doi.org/10.1016/j.meegid.2012.11.015
7. Trojnar E, Otto P, Roth B, Reetz J, Johne R. The genome segments of a group D rotavirus possess group A–like conserved termini but encode group-specific proteins. J Virol. 2010;84:10254–65. http://dx.doi.org/10.1128/JVI.00332-10
8. Roy A, Kucukural A, Zhang Y. I-TASSER: a unified platform for automated protein structure and function prediction. Nat Protoc. 2010;5:725–38. http://dx.doi.org/10.1038/nprot.2010.5
9. Mathieu M, Petitpas I, Navaza J, Lepault J, Kohli E, Pothier P, et al. Atomic structure of the major capsid protein of rotavirus: implications for the architecture of the virion. EMBO J. 2001;20:1485–97. http://dx.doi.org/10.1093/emboj/20.7.1485
10. Matthijnssens J, Ciarlet M, McDonald SM, Attoui H, Bányai K, Brister JR, et al. Uniformity of rotavirus strain nomenclature proposed by the Rotavirus Classification Working Group (RCWG). Arch Virol. 2011;156:1397–413. http://dx.doi.org/10.1007/s00705-011-1006-z
11. Matthijnssens J, Ciarlet M, Heiman E, Arijs I, Delbeke T, McDonald SM, et al. Full genome-based classification of rotaviruses reveals a common origin between human Wa-Like and porcine rotavirus strains and human DS-1–like and bovine rotavirus strains. J Virol. 2008;82:3204–19. http://dx.doi.org/10.1128/JVI.02257-07
12. Marthaler D, Rossow K, Gramer M, Collins J, Goyal S, Tsunemitsu H, et al. Detection of substantial porcine group B rotavirus genetic diversity in the United States, resulting in a modified classification proposal for G genotypes. Virology. 2012;433:85–96. http://dx.doi.org/10.1016/j.virol.2012.07.006
13. Wakuda M, Ide T, Sasaki J, Komoto S, Ishii J, Sanekata T, et al. Porcine rotavirus closely related to novel group of human rotaviruses. Emerg Infect Dis. 2011;17:1491–3.
14. Esona MD, Mijatovic-Rustempasic S, Conrardy C, Tong S, Kuzmin IV, Agwanda B, et al. Reassortant group A rotavirus from straw-colored fruit bat (*Eidolon helvum*). Emerg Infect Dis. 2010;16:1844–52. http://dx.doi.org/10.3201/eid1612.101089

Address for correspondence: Krisztián Bányai, Institute for Veterinary Medical Research, Centre for Agricultural Research, Hungarian Academy of Sciences, H-1143 Budapest, Hungária krt. 21, Hungary; email: bkrota@hotmail.com

Article DOI: http://dx.doi.org/10.3201/eid2104.141370

Candidate New Rotavirus Species in Sheltered Dogs, Hungary

Technical Appendix

Technical Appendix Table 1. Comparison of the genome size and the coding potential of different rotavirus species*

Genome segment	*Rotavirus A*, Wa		*Rotavirus A*, 02V0002G3		*Rotavirus B*, Bang373		*Rotavirus C*, Bristol		*Rotavirus D*, 05V0049	
	Length, nt	Protein (aa)	Length, nt	Protein (aa)	Length, nt	Protein (aa)	Length, nt	Protein (aa)	Length, nt	Protein (aa)
1	3302	VP1 (1088)	3305	VP1 (1089)	3511	VP1 (1160)	3309	VP1 (1090)	3274	VP1 (1079)
2	2717	VP2 (890)	2732	VP2 (895)	2847	VP2 (934)	2736	VP2 (884)	2801	VP2 (913)
3	2591	VP3 (835)	2583	VP3 (829)	2341	VP3 (763)	2283	VP3 (693)	2366	VP4 (777)
4	2359	VP4 (775)	2354	VP4 (770)	2306	VP4 (750)	2166	VP4 (744)	2104	VP3 (685)
5	1567	NSP1 (486)	2122	NSP1 (577)	1276	NSP1–1 (107) NSP1–2 (321) NSP1–3 (65)	1353	VP6 (395)	1872	NSP1 (574)
6	1356	VP6 (397)	1348	VP6 (397)	1269	VP6 (391)	1350	NSP3 (402)	1353	VP6 (398)
7	1074	NSP3 (310)	1089	NSP3 (304)	1179	NSP3 (347)	1270	VP6 (394)	1242	NSP3 (370)
8	1062	VP7 (326)	1066	VP7 (329)	1007	NSP2 (301)	1063	VP7 (332)	1026	NSP2 (310)
9	1059	NSP2 (317)	1042	NSP2 (315)	814	VP7 (249)	1037	NSP2 (312)	1025	VP7 (316)
10	750	NSP4 (175)	724	NSP4 (168)	751	NSP4 (219)	730	NSP5 (212)	765	NSP4 (127) ORF2 (93)
11	664	NSP5 (197) NSP6 (92)	699	NSP5 (208)	631	NSP5 (170)	615	NSP4 (150)	672	NSP5 (195)
Sum	18,501		19,064		17,932		17,912		18,500	
Genome segment	*Rotavirus F*, 03V0568		*Rotavirus G*, 03V0567		*Rotavirus H*, J19		*Rotavirus I*, KE135/2012		*Rotavirus I*, KE528/2012	
	Length, nt	Protein (aa)	Length, nt	Protein (aa)	Length, nt	Protein (aa)	Length, nt	Protein (aa)	Length, nt	Protein (aa)
1	3296	VP1 (1086)	3526	VP1 (1160)	3538	VP1 (1167)	3518	VP1 (1162)	3518	VP1 (1162)
2	2769	VP2 (904)	3014	VP2 (991)	2969	VP2 (973)	3002	VP2 (982)	3000	VP2 (982)
3	2246	VP4 (738)	2364	VP4 (772)	2512	VP4 (823)	2371	VP4 (777)	2370	VP4 (777)
4	2174	VP3 (694)	2352	VP3 (768)	2204	VP3 (719)	2161	VP3 (701)	2162	VP3 (701)
5	1791	NSP1 (547)	1295	NSP1–1 (106) NSP1–2 (324)	1307	NSP1 (395)	1485	NSP1–1 (79) NSP1–2 (390)	1484	NSP1–1 (79) NSP1–2 (390)
6	1314	VP6 (396)	1267	VP6 (391)	1287	VP6 (396)	1278	VP6 (395)	1279	VP6 (395)
7	1309	NSP3 (370)	1052	NSP3 (300)	1004	NSP3 (297)	1018	NSP2 (301)	1016	NSP2 (301)
8	1068	NSP2 (318)	1012	NSP2 (282)	932	NSP2 (262)	954	NSP3 (273)	951	NSP3 (273)
9	990	VP7 (295)	825	VP7 (247)	820	VP7 (258)	858	VP7 (268)	869	VP7 (273)
10	706	NSP5 (218)	801	NSP4 (187)	739	NSP4 (213)	751	NSP4 (219)	750	NSP4 (219)
11	678	NSP4 (169 aa)	678	NSP5 (181)	649	NSP5 (176)	593	NSP5 (157)	589	NSP5 (157)
Sum	18,341		18,186		17,961		17,989		17,988	

*Rotavirus species and type strain is shown in the upper row. The coding regions were predicted using the ORF Finder program (http://www.ncbi.nlm.nih.gov/gorf/gorf.html).

Laboratory Methods

Semiconductor Sequencing

Ten percent fecal suspensions were prepared in phosphate buffered saline and then centrifuged at 5000 × g for 10 min. Viral RNA was extracted by using the Zymo DirectZol kit (Zymo Research, Orange, CA, USA) combined with the RiboZol RNA extraction ragent (Amresco, Solon, OH, USA), according to the protocol recommended by the manufacturer for biological liquids, although DNase treatment was omitted from the workflow.

The RNA sample was subsequently denatured at 97°C for 5 min in the presence of 10 μM random hexamer tailed by a common PCR primer sequence (*1*). Reverse transcription was performed with 1 U AMV reverse transcriptase (Promega, Madison, WI, USA), 400 μM dNTP mixture, and 1× AMV RT buffer at 42°C for 45 min following a 5-min incubation at room temperature. Then, 5 μL cDNA was added to 45 μL PCR mixture to obtain a final volume of 50 μL and a concentration of 500 μM for the PCR primer, 200 μM for dNTP mixture, 1.5 mM for $MgCl_2$, 1× Taq DNA polymerase buffer, and 0.5 U for Taq DNA polymerase (Thermo Scientific, Vilnius, Lithuania). The reaction conditions consisted of an initial denaturation step at 95°C for 3 min, followed by 40 cycles of amplification (95°C for 30 sec, 48°C for 30 sec, 72°C for 2 min) and terminated at 72°C for 8 min.

We subjected 0.1 μg of cDNA to enzymatic fragmentation and adaptor ligation (NEBNext Fast DNA Fragmentation & Library Prep Set for Ion Torrent kit, New England Biolabs, Ipswich, MA, USA). The barcoded adaptors were retrieved from the Ion Xpress Barcode Adapters (Life Technologies, Carlsbad, CA, USA). The resulting cDNA libraries were measured on an Qubit 2.0 device using the Qubit dsDNA BR Assay kit (Invitrogen, Eugene, OR, USA). The emulsion PCR that produced clonally amplified libraries was carried out according to the manufacturer's protocol using the Ion PGM Template kit on an OneTouch v2 instrument. Enrichment of the templated beads (on an Ion One Touch ES machine) and further steps of presequencing setup were performed according to the

200-bp protocol of the manufacturer. The sequencing protocol recommended for Ion PGM Sequencing Kit on an 316 chip was strictly followed (*2*,*3*).

Determination of the Termini of Genomic RNA

To obtain the true sequence of the genome segment ends, a short oligonucleotide (PC3), phosphorylated at the 5′ end and blocked at the 3′ end with dideoxy cytosine, was ligated to the 3′ ends of the genomic RNA in the nucleic acid extract (*4*,*5*). In brief, 5 μL total RNA was combined with 25 μL RNA ligation mixture (consisting of 3.5 μL nuclease free water, 2 μL of 20 μM PC3, 12.5 μL of 34% (w/v) polyethylene glycol 8000, 3 μL ATP, 3 μL 10X T4 RNA Ligase buffer and 10 U T4 RNA Ligase I (New England Biolabs, Ipswich, MA, USA) and then incubated at 17°C for 16 h. Following the incubation, the RNA was extracted by using the QIAquick Gel Extraction Kit (QIAGEN, Hilden, Germany). Binding of RNA to silica-gel column was performed in the presence of 150 μL QG buffer from the extraction kit and 180 μL isopropanol. All subsequent steps were performed according to the manufacturer's instructions.

Five microliters ligated RNA was heat-denatured in the presence of 1 μL of 20 μM primer (PC2, which is complementary to the PC3 oligonucleotide ligated to the 3′ end) at 95°C for 5 min and then placed on ice slurry. The reverse transcription mixture contained 14 μL nuclease free water, 6 μL 5× First Strand Buffer, 1 μL of 10 μM dNTP mixture, 1 μL 0.1M dTT, 20 U RiboLock RNase Inhibitor (Thermo Scientific, Vilnius, Lithuania), and 300 U SuperScript III Reverse Transcriptase (Invitrogen, Eugene, OR, USA). This mixture was added to the denatured ligated RNA and incubated at 25°C for 5 min and then 50°C for 60 min. The reaction was stopped at 70°C for 15 min (*6*).

Subsequently, 2 μL cDNA was added to the PCR mixture, which consisted of 17 μL nuclease-free water, 1 μL of 10 μM dNTP mixture, 2,5 μL 10× DreamTaq Green Buffer (including 20 mM $MgCl_2$), and 2 μL of 20 μM primer pair (i.e., 1 μL PC2 and 1 μL gene-specific primer; data not shown) and 2.5 U DreamTaq DNA polymerase (Thermo Scientific, Vilnius, Lithuania). The thermal profile consisted of the following steps: 95°C 3 min 40 cycles of 95°C 30 sec, 42°C 30 sec. 72°C 2 min final elongation at 72°C for 8

min. The PCR products were visualized on 1% agarose gel electrophoresis, and bands of the expected sizes were excised and cleaned up with Geneaid Gel/PCR DNA fragments Extraction Kit (Geneaid, Taipei, Taiwan).

Subsequently, amplicons were subjected to Sanger sequencing with the PCR primers by using the BigDye Terminator v1.1 Cycle Sequencing Kit (Applied Biosystems, Austin, TX, USA). Ethanol precipitated products were run on an ABI PRISM 310 Genetic Analyzer.

Sanger Sequencing of the VP7 Gene

Because of the significant sequence heterogeneity identified between the VP7 gene of KE135/2012 and KE528/2012, it seemed relevant to confirm the semiconductor sequencing results by using traditional sequencing. Therefore, the whole-genome segment encoding the VP7 gene was sequenced for both strains. cDNA production, amplification and Sanger sequencing were carried out with sequence specific primers (data not shown) designed based on the Ion Torrent sequence reads. The experimental protocol was essentially the same as described in the previous section describing the determination of genome segment termini.

Reference List for the Laboratory Methods Section.

1. Djikeng A, Halpin R, Kuzmickas R, Depasse J, Feldblyum J, Sengamalay N, et al. Viral genome sequencing by random priming methods. BMC Genomics. 2008;9:5. PubMed http://dx.doi.org/10.1186/1471-2164-9-5

2. Papp H, Marton S, Farkas SL, Jakab F, Martella V, Malik YS, et al. Classification and characterization of a laboratory chicken rotavirus strain carrying G7P[35] neutralization antigens on the genotype 4 backbone gene configuration. Biologicals. 10.1016/j.biologicals.2014.08.004. PubMed

3. Dóró R, Mihalov-Kovács E, Marton S, László B, Deák J, Jakab F, et al. Large-scale whole genome sequencing identifies country-wide spread of an emerging G9P[8] rotavirus strain in Hungary, 2012. Infect Genet Evol. 2014;28:495–512. PubMed http://dx.doi.org/10.1016/j.meegid.2014.09.016

4. Lambden PR, Cooke SJ, Caul EO, Clarke IN. Cloning of noncultivatable human rotavirus by single primer amplification. J Virol. 1992;66:1817–22. PubMed

5. Potgieter AC, Page NA, Liebenberg J, Wright IM, Landt O, van Dijk AA. Improved strategies for sequence-independent amplification and sequencing of viral dsRNA genomes. J Gen Virol. 2009;90:1423–32. PubMed http://dx.doi.org/10.1099/vir.0.009381-0

6. Bányai K, Dandár E, Dorsey KM, Mató T, Palya V. The genomic constellation of a novel avian orthoreovirus strain associated with runting-stunting syndrome in broilers. Virus Genes. 2011;42:82–9. PubMed http://dx.doi.org/10.1007/s11262-010-0550-z

Technical Appendix Table 2. Percentile nucleotide (nt) and amino acid (aa) sequence based identities between the novel canine rotavirus (RV) strain, KE135/2012, and reference RVA-RVD and RVF-RVH strains*

	RVA		RVB		RVC		RVD		RVF		RVG		RVH	
Gene	nt	aa	nt	aa	nt	aa	nt	aa	nt	aa	nt	aa	nt	aa
VP1	40–41	24	57–59	53–54	40–41	23	41	23	42	24	60–61	55	61–62	57–58
VP2	36	15	51–52	42	37–38	15	36	13	38	15	53	41	55–56	46
VP3	38–40	17	49–50	32	37–38	16–17	38	18	38	17	47–48	32–33	52	38–39
VP4	36–37	14–15	43	24–27	36	14–16	36	15	38	15	43–45	25–28	42	24–26
VP6	33–34	14–15	49–50	37	36–37	17–18	37	16	33	12	49–52	35–37	54	45–46
VP7†	38–39	18–20	46–48	29	35–36	16	37	17	37	15	43–45	24–26	44–45	27–28
NSP1	31–32	11	35–37	15–16	32–33	<10	34	13	34	11	38–39	18–20	48	30
NSP2	36–37	19–20	52–53	42	38	20	39	19	37	20	52–53	39–41	52	41
NSP3	38–39	18–19	42	24–26	36–37	14	39	19	34	14	43	19–22	40	20
NSP4‡	35–39	10–15	35–39	15	35–39	14–15	35	11	40	19	36–38	17	37	14–15
NSP5	33–34	10–11	45–46	24–27	32–33	10–12	30	11	35	12	46–48	27–30	47–48	28–29

*The Muscle algorithm within the Translator X (*1*) online platform was used to obtain codon-based multiple alignments. Nucleotide and deduced amino acid sequence alignments were visualized in GeneDoc (*2*), whereas sequence distances were calculated with the MEGA6 program using the P distance algorithm (*3*). Results obtained by this method were used to calculate sequence identity values.
†The VP7 gene was sequenced for both RVI strains by traditional methods as well. Of note is that Ion Torrent and Sanger sequencing results were congruent.
‡Assignment of the NSP4 was not possible by homology search. However, structure-based analysis identified putative helical transmembrane (site aa 47–64 and/or 71–88) and coiled coil region (site aa 142–168) and predicted a glycosylation site (motif, NGS; site aa 31).

References to Technical Appendix Table 2

1. Abascal F, Zardoya R, Telford MJ. TranslatorX: multiple alignment of nucleotide sequences guided by amino acid translations. Nucleic Acids Res. 2010;38:W7–13. PubMed http://dx.doi.org/10.1093/nar/gkq291

2. Nicholas KB, Nicholas HB Jr, Deerfield DW II. GeneDoc: analysis and visualization of genetic variation. Embnet News. 1997;4:14.

3. Tamura K, Stecher G, Peterson D, Filipski A, Kumar S. MEGA6: Molecular Evolutionary Genetics Analysis version 6.0. Mol Biol Evol. 2013;30:2725–9. PubMed http://dx.doi.org/10.1093/molbev/mst197

The 5′ end sequence of the VP2 gene of KE528/2012

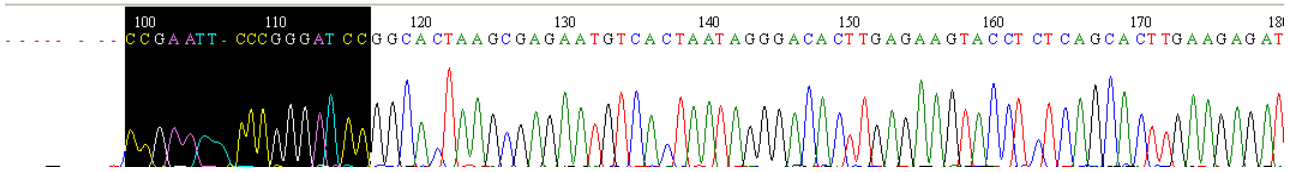

The 3′ end sequence of the VP2 gene of KE528/2012

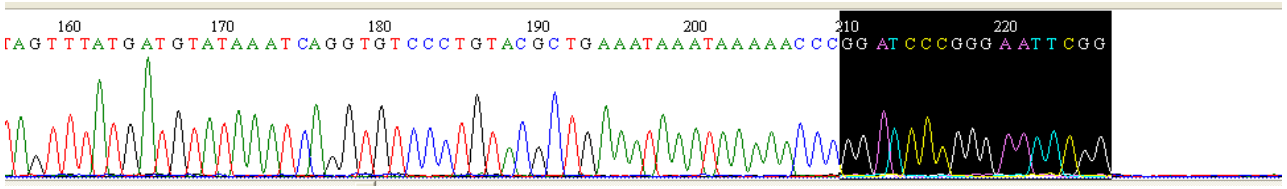

Technical Appendix Figure 1. 5′ and 3′ termini confirmed by Sanger sequencing. To illustrate the sequencing results, an example is inserted below. The ligated oligonucleotide sequence at the 3′ ends of the genomic RNA is shown with dark background. Please note that numbers above the peaks indicate the base position in the chromatogram and not the base position in the genome segment.

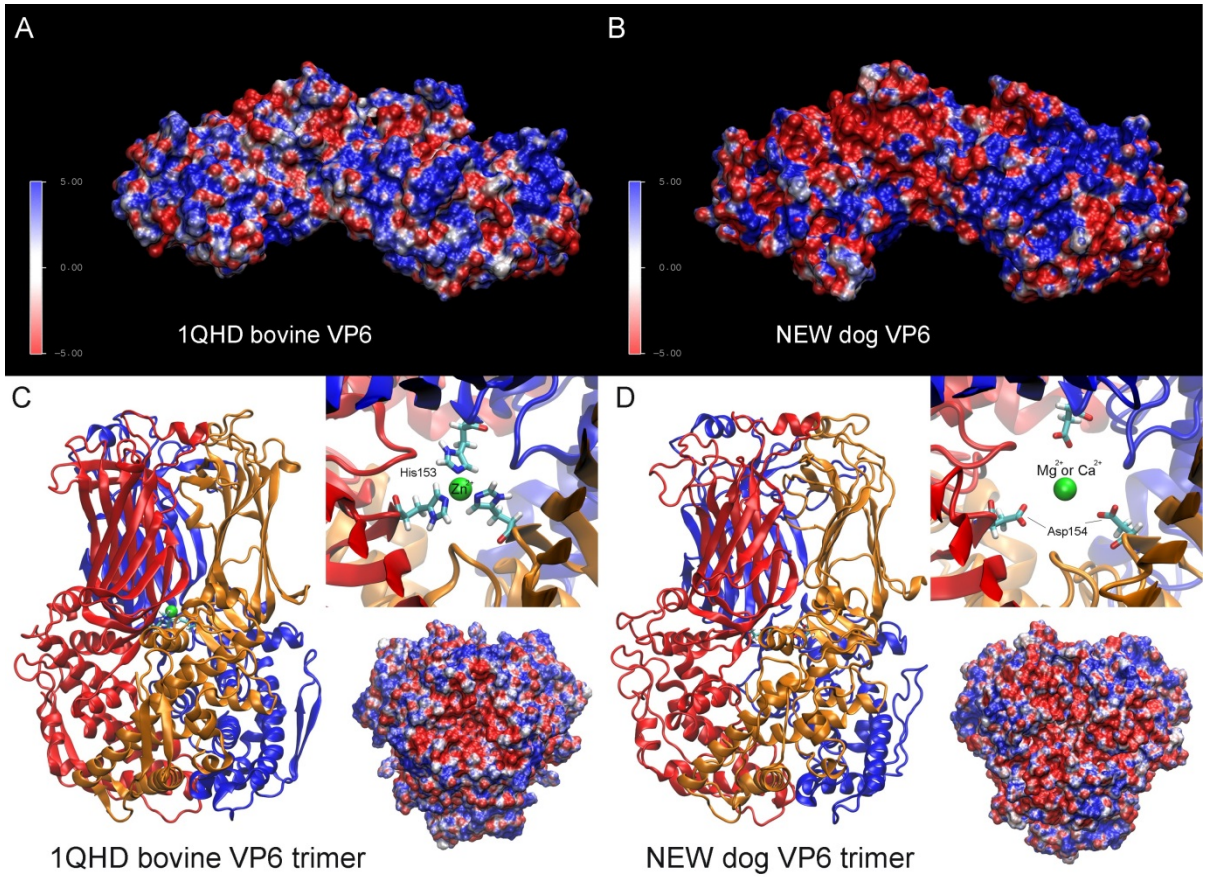

Technical Appendix Figure 2. Additional insight into the structure of the VP6 protein and its homotrimer form. The protein structure was generated with I-TASSER (*1*) by using the following experimentally determined templates (referring PDB ID codes): 1QHD (VP6, bovine RVA strain RF), 3KZ4 (VP6, bovine RVA strain UK), 3SMT (Human SET domain-containing protein3), 1B5Q (Polyamine oxidase from *Zea mays*), 1XPQ (Polyamine oxidase from yeast) and 1SEZ (Protoporphyrinogen IX oxidase from tobacco). A VP6 trimer was created from the generated VP6 model using the biologic assembly coordinate of the main template, the bovine RVA VP6 protein trimer (PDB ID: 1QHD). The model structures were refined with the Schrödinger molecular modeling software package (*2*) to eliminate the steric conflicts between the protein side chain atoms. Pairwise protein sequence alignment was calculated with the NeedleP tool of the SRS bioinformatics software package. Electrostatic

potential maps were calculated with Adaptive Poisson–Boltzmann Solver (APBS) version 1.3 by using the linearized Poisson–Boltzmann method with a dielectric constant of 78 and 2 for the water solvent and protein core, respectively. The partial charges for the electrostatic potential calculations were calculated with PDB2PQR (*3*–*5*). Molecular graphics and sequence alignment visualization were prepared by using VMD version 1.9.1 and the Multiple Sequence Viewer of the Schrödinger Suite, respectively (*6*). Electrostatic view of the bovine VP6 (A) and the new canine VP6 (B) rotavirus coat protein surfaces. Colors: red, regions with potential value less than –5.0 kT; white, 0.0; blue, greater than +5.0 kT. Comparison between bovine (C) and the canine (D) VP6 trimers. The central metal ion binding sites are indicated on the right top insets of C and D. The outer antigenic surface of the VP6 trimers (right lower insets) are colored by electrostatic potential distribution. Previous studies demonstrated that the RVA VP6 trimer is stabilized by Zn^{2+} located at the center of the complex on the 3-fold axis (C). The bound Zn^{2+} is coordinated by His153 from each of the 3 VP6 subunits. Interestingly, the novel canine rotavirus VP6 protein possessed no His around this location. Instead, a negatively charged amino acid residue, Asp, was found in position 154. Negatively charged amino acids (such as Asp and Glu) usually take part in Mg^{2+}, Mn^{2+} and Ca^{2+} ion coordination but not Zn^{2+} ion. Based on this finding we assume that a metal ion other than Zn^{2+} (e.g., Mg^{2+} or Ca^{2+}) may be coordinated by Asp154 in the center of the canine RVI VP6 capsomere to stabilize the trimer form (Panel D). The question whether if this finding might have implications for virion stability or resource use within the infected cell during virion assembly is open.

Reference List for Technical Appendix Figure 2

1. Zhang Y. I-TASSER server for protein 3D structure prediction. BMC Bioinformatics. 2008;9:40. PubMed http://dx.doi.org/10.1186/1471-2105-9-40

2. Suite S. New York: Schrödinger, LLC; 2013.

3. Baker NA, Sept D, Joseph S, Holst MJ, McCammon JA. Electrostatics of nanosystems: application to microtubules and the ribosome. Proc Natl Acad Sci U S A. 2001;98:10037–41. PubMed http://dx.doi.org/10.1073/pnas.181342398

4. Gilson MK, Sharp KA, Honig B. Calculating electrostatic interactions in biomolecules: method and error assessment. J Comput Chem. 1987;9:327–35. http://dx.doi.org/10.1002/jcc.540090407

5. Dolinsky TJ, Nielsen JE, McCammon JA, Baker NA. PDB2PQR: an automated pipeline for the setup, execution, and analysis of Poisson-Boltzmann electrostatics calculations. Nucleic Acids Res. 2004;32(Web Server issue):W665–7.

6. Humphrey W, Dalke A, Schulten K. VMD - Visual Molecular Dynamics. J Mol Graph. 1996;14:33–8. PubMed http://dx.doi.org/10.1016/0263-7855(96)00018-5

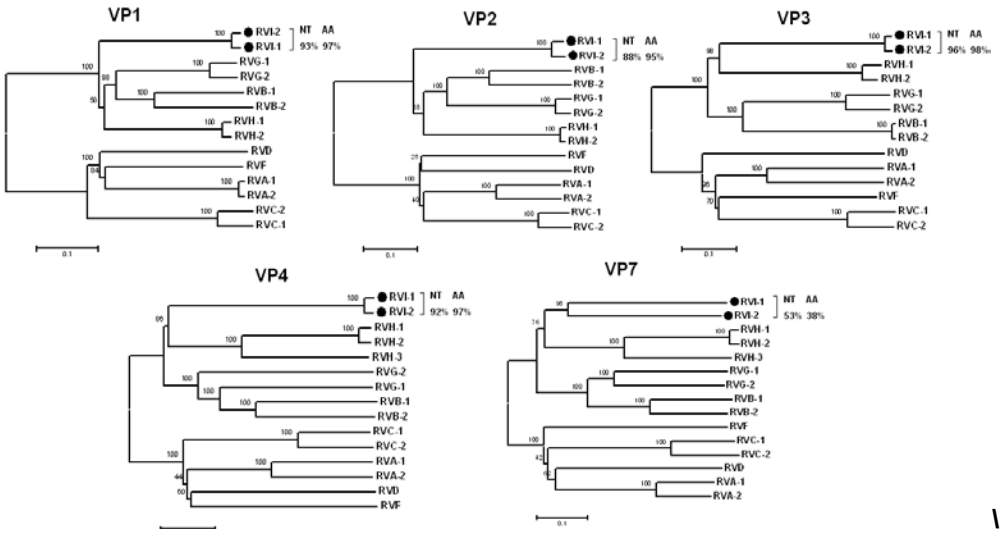
VP1
RVI-2
RVI-1
NT AA
93% 97%
RVG-1
RVG-2
RVB-1
RVB-2
RVH-1
RVH-2
RVD
RVF
RVA-1
RVA-2
RVC-2
RVC-1
VP2
RVI-1
RVI-2
NT AA
88% 95%
RVB-1
RVB-2
RVG-1
RVG-2
RVH-1
RVH-2
RVF
RVD
RVA-1
RVA-2
RVC-1
RVC-2
VP3
RVI-1
RVI-2
NT AA
96% 98%
RVH-1
RVH-2
RVG-1
RVG-2
RVB-1
RVB-2
RVD
RVA-1
RVA-2
RVF
RVC-1
RVC-2
VP4
RVI-1
RVI-2
NT AA
92% 97%
RVH-1
RVH-2
RVH-3
RVG-2
RVG-1
RVB-1
RVB-2
RVC-1
RVC-2
RVA-1
RVA-2
RVD
RVF
VP7
RVI-1
RVI-2
NT AA
53% 38%
RVH-1
RVH-2
RVH-3
RVG-1
RVG-2
RVB-1
RVB-2
RVF
RVC-1
RVC-2
RVD
RVA-1
RVA-2

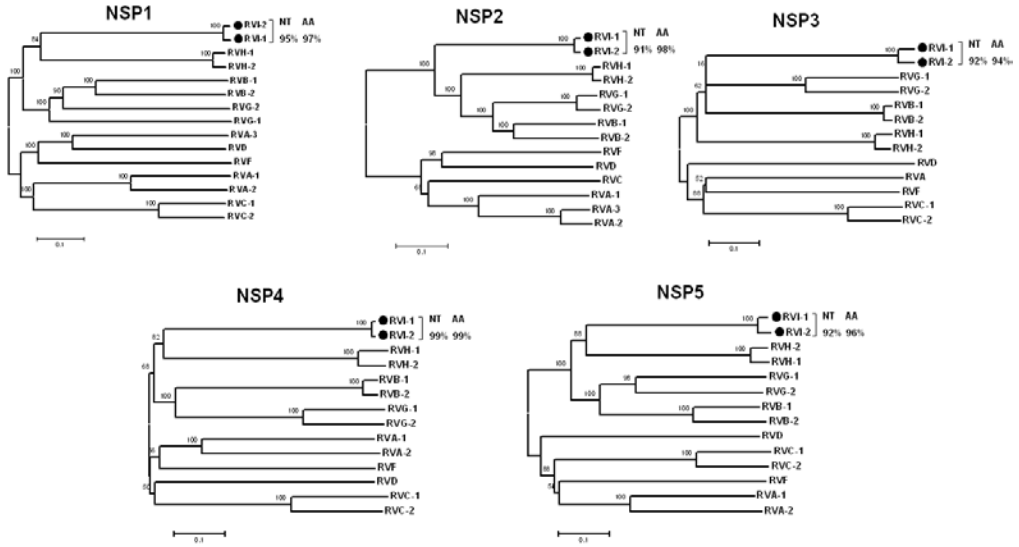
NSP1
RVI-2
RVI-1
NT AA
95% 97%
RVH-1
RVH-2
RVB-1
RVB-2
RVG-2
RVG-1
RVA-3
RVD
RVF
RVA-1
RVA-2
RVC-1
RVC-2
NSP2
RVI-1
RVI-2
NT AA
91% 98%
RVH-1
RVH-2
RVG-1
RVG-2
RVB-1
RVB-2
RVF
RVD
RVC
RVA-1
RVA-3
RVA-2
NSP3
RVI-1
RVI-2
NT AA
92% 94%
RVG-1
RVG-2
RVB-1
RVB-2
RVH-1
RVH-2
RVD
RVA
RVF
RVC-1
RVC-2
NSP4
RVI-1
RVI-2
NT AA
99% 99%
RVH-1
RVH-2
RVB-1
RVB-2
RVG-1
RVG-2
RVA-1
RVA-2
RVF
RVD
RVC-1
RVC-2
NSP5
RVI-1
RVI-2
NT AA
92% 96%
RVH-2
RVH-1
RVG-1
RVG-2
RVB-1
RVB-2
RVD
RVC-1
RVC-2
RVF
RVA-1
RVA-2

Technical Appendix Figure 3. Phylogenetic trees obtained for the VP1 to VP4, VP7, NSP1 to NSP5 proteins with representative strains of RVA to RVH. RVI-1, and RVI-2 represents KE135/2012 and KE528/2012, respectively. Alignments were created by using the BLOSUM62 algorithm as implemented at the Multalin website (http://multalin.toulouse.inra.fr/multalin/). Phylogenetic trees were prepared by using the neighbor-joining method. Bootstrap values are shown at the branch nodes. Nucleotide and amino acid identities between KE135/2012 and KE528/2014 are show on the right. Of note is the low sequence homology within the VP7 of RVI strains, KE135/2012 and KE528/2014. Such limited VP7 sequence identity values classify RVA-RVC rotaviruses into different G genotypes. Therefore, we tentatively assigned the 2 RVI strains into 2 different G types, G1 and G2 (see the main text). In the other genes, the RVI strains in our study most likely share the respective genotype specificity.

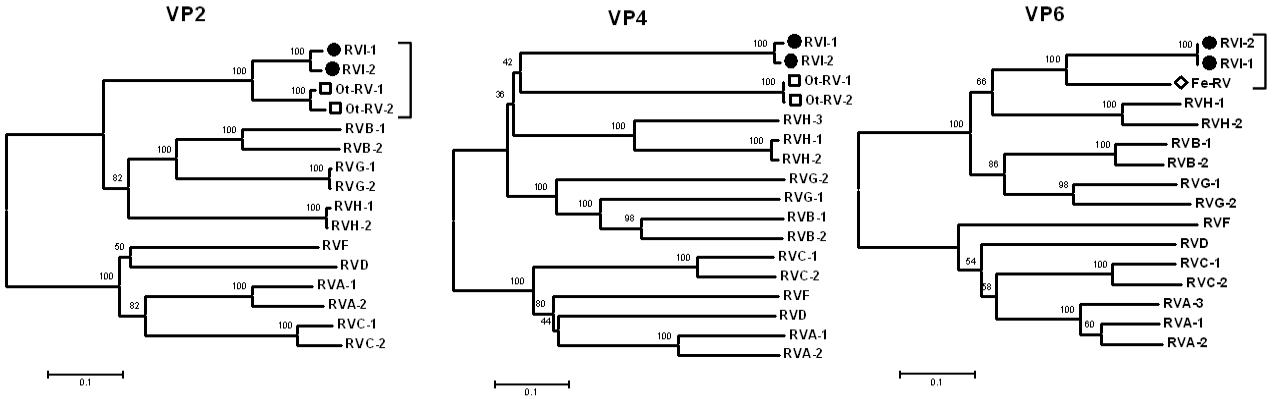

Technical Appendix Figure 4. Phylogenetic trees obtained for the partial sequences using unusual feline and otarine RV gene sequences. The alignments of the VP2, VP4, and VP6 proteins encompassed ≈160, ≈310, and ≈70 aa long sequences.